



**Nucleation and Nonisothermal Crystallization Kinetics in  
Cross-linked Polyethylene/Zinc Oxide Nanocomposites**

|                               |                                                                                                                                                                                                                                                                                                                                        |
|-------------------------------|----------------------------------------------------------------------------------------------------------------------------------------------------------------------------------------------------------------------------------------------------------------------------------------------------------------------------------------|
| Journal:                      | <i>RSC Advances</i>                                                                                                                                                                                                                                                                                                                    |
| Manuscript ID:                | RA-ART-04-2014-003731.R1                                                                                                                                                                                                                                                                                                               |
| Article Type:                 | Paper                                                                                                                                                                                                                                                                                                                                  |
| Date Submitted by the Author: | 22-Jun-2014                                                                                                                                                                                                                                                                                                                            |
| Complete List of Authors:     | Jose, Josmin; Mahatma Gandhi University, School of Chemical Sciences Chazeau, Laurent; INSA Lyon, France, MATEIS, INSA Lyon & CNRS, Cavaillé, Jean-Yves; INSA Lyon, France, MATEIS, INSA Lyon & CNRS K. T., Varughese; Central Power Research Institute, Hyderabad, Thomas, Sabu; mahatmagandhi university, School of Chemical Science |
|                               |                                                                                                                                                                                                                                                                                                                                        |

## Nucleation and Nonisothermal Crystallization Kinetics in Cross-linked Polyethylene/Zinc Oxide Nanocomposites

Josmin P. Jose<sup>1 a</sup>, Laurent Chazeau<sup>2</sup>, Jean-Yves Cavaille<sup>2</sup>, K. T. Varughese<sup>3</sup>, Sabu Thomas\*<sup>4 b</sup>

<sup>1</sup> School of Chemical Sciences, Mahatma Gandhi University, Kottayam, Kerala, India, 686 560

<sup>2</sup> MATEIS, INSA Lyon & CNRS, UMR 5510, 69621 Villeurbanne cedex, France

<sup>3</sup> Dielectric Material Division, Central Power Research Institute, Bangalore, India, 560080

<sup>4</sup> School of Chemical Sciences, Mahatma Gandhi University, Kottayam, Kerala, India; Jozef Stefan Institute, Department F4 Jamova Cesta 39 SI-1000, Ljubljana, Slovenia; Universiti of Teknologi MARA, 40450, Shah Alam, Selangor, Malaysia; Centre for Nanoscience and Nanotechnology, Mahatma Gandhi University, Kottayam, Kerala, India, 686560

<sup>a</sup>[josminroselite@gmail.com](mailto:josminroselite@gmail.com), <sup>b</sup>[sabupolymer@yahoo.com](mailto:sabupolymer@yahoo.com),

### Abstract

In the present study organic-inorganic hybrid nanocomposites of cross linked polyethylene (XLPE) with 0, 2, 5 and 10 wt % of trimethoxyoctyl-silane surface treated ZnO nanoparticles were prepared by melt mixing. Non isothermal crystallization kinetics is performed in detail to reveal the crystallization characteristics of a cross linked system (XLPE) in the presence of nanomaterials (ZnO) as dispersed phase. Based on the diffusion controlled growth theory, all the nanocomposites of the present system, exhibit constant nucleation rate or the growth of nanometer aggregates that constitutes nuclei, with an increasing nucleation rate. Non isothermal crystallization kinetic parameters and the theoretical estimation of nucleation activity certify the nucleating capability of ZnO nano materials in the cross-linked continuous phase of XLPE. The experimental results confirmed that, even at very fast cooling rates, the promising role of nano particle for nucleation is able to compensate the negative effect of fast cooling.

*Key words:* Cross linked polyethylene, nano ZnO, nonisothermal crystallization, heterogeneous nucleation, nucleation activity, activation energy

### 1. Introduction

In all industrial processes, pressure and temperature change very quickly, which in the case of semi crystalline polymers induces very different crystallization conditions and further different morphologies, volume fraction, type of crystalline phase which in turn lead to different mechanical properties.<sup>1-4</sup> Therefore the study of crystallization behavior in a

continuously changing environment is of great interest.<sup>5-7</sup> This type of study generally proceeds under non-isothermal conditions.<sup>8</sup>

Since organic-inorganic hybrid composite material is having excellent mechanics by combining the advantages of polymeric matrix with the unique characteristics of the inorganic nanoparticles, it is crucial to analyze the crystallization characteristics of such systems to reveal the microstructure and morphology.<sup>9-10</sup> One of the main challenges in the field of hybrid composites is the difficulty in proper dispersion of inorganic nanoparticles in polymers due to the incompatibility in surface characteristics between organic, hydrophobic, non polar polymer and inorganic, hydrophilic, polar nanofillers. The use of surface modification agents on nanofillers is required to solve this problem.<sup>11-12</sup> It is worthy to notice that many works claim large improvement of polymer mechanical stiffness with the addition of very small amount of fillers. Such stiffness increases cannot be explained as a simple mechanical reinforcement, as shown by classical mechanical coupling equations. So it is essential to search the change in mobility and orientation of polymer chains in the presence of nanoparticles. In fact, a well dispersed minor phase of nanomaterials can affect the crystallization characteristics of its continuous polymeric matrix, since it creates a very large interfacial area.<sup>7</sup> According to the classical approach and also to simulation calculation, solid surfaces present in a polymer melt induce heterogeneous nucleation, due to reduced free energy for nucleation at the melt/solid interface.<sup>13-15</sup> Thus nanofillers may act as nucleating agents and therefore may improve the crystallization rate.

For instance, it has been reported that crystallization rate of polyethylene can be enhanced in the presence of various nucleating agents<sup>4</sup>. Olmos *et al.*<sup>1</sup> have investigated crystallization and final morphology of HDPE/TiO<sub>2</sub> nanocomposites. They optimized the amount of nano fillers, which can contribute to heterogeneous crystallization. Nucleation activation and spherical crystal morphology of LLDPE/LDPE/TiO<sub>2</sub> nanocomposites prepared by non-isothermal crystallization study was done by Wang *et al.*<sup>3</sup> and they highlighted the effect of cooling rate on heterogeneous nucleation. Abbasi *et al.*<sup>2</sup> reported the effect of aspect ratio and chemical modification of multi walled carbon nanotubes on the non-isothermal crystallization kinetics. The crystallization onset temperature and crystallization peak temperature were significantly affected by the amount of multi walled carbon nanotube (MWCNT).

Thus, it is of great interest to investigate the crystallization behavior of polymer nanocomposites, since the presence of nanofiller affects the crystalline structure, morphology and therefore the final physical properties of this materials.<sup>16-17</sup> In the present article non-isothermal crystallization kinetics of Cross-linked polyethylene/ZnO hybrid nanocomposites were investigated. The heterogeneous nucleating capability of ZnO nanoparticles in a semi-crystalline, cross-linked polymer is a new research problem and to the author's knowledge has never been addressed. It is expected that the research reported herein will be of interest for a better understanding of the microstructural change

in the XLPE continuous phase in the vicinity of ZnO nano materials and of its kinetics of crystallization.

## **2. Experimental:**

### **2.1 Materials**

Low density polyethylene (PETROTHENE NA951080), with a density of 0.94 g/cm<sup>3</sup> was obtained from Equistar, USA. The cross linking agent dicumyl peroxide (DCP) and antioxidant Irganox 1010 were used. The nano ZnO with 100 % silane, trimethoxyoctyl-reaction product, having 20 nm in diameter was obtained from Evonik Industries, United States.

### **2.2 Nanocomposite Fabrication**

XLPE/ZnO nanocomposites were prepared by melt mixing using dicumyl peroxide as the curing agent. The nanocomposites with 0, 2, 5 and 10 wt. % ZnO were prepared. The cross linking agent, DCP 1.5 wt. % and antioxidant 0.5 wt. % were used. The mixing was done in a Haake mixer at 160 °C and 60 rpm for 12 minutes. The temperature, rotation speed, time of mixing and the amount of DCP and Irganox were kept constant for all mixes. These parameters have been selected based on the previous findings on this system. The mixed nanocomposites were compression molded in a SHP-30 model hydraulic press with a maximum pressure of 200 kg/cm<sup>2</sup> at 180 °C for 5 minutes. High pressure was applied while molding, otherwise the escaped methane, the cross linking by-product will form pores in the films. Nanocomposites with 2, 5 and 10 wt. % ZnO content were designated as Z<sub>2</sub>, Z<sub>5</sub> and Z<sub>10</sub>. Composite of XLPE without nanofiller, designated as X was also prepared for comparison.

### **2.3 Characterizations**

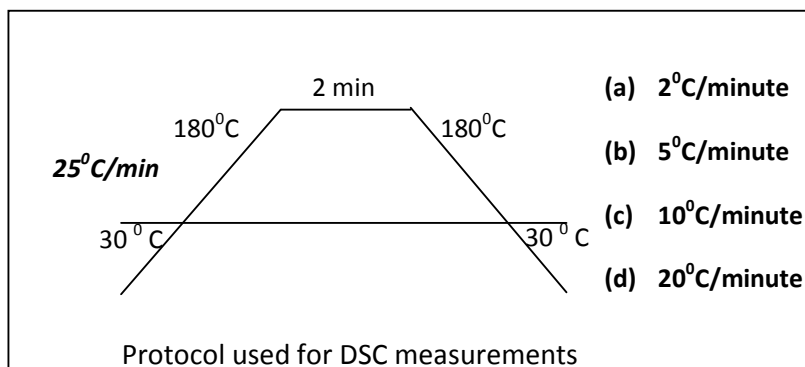
#### **2.3.1 Morphological Analysis**

The filler dispersion in the polymer matrix was investigated using TEM. The micrographs of the nanocomposites were taken in JEOL JEM transmission electron microscope with an accelerating voltage of 200 kV. Ultrathin sections of bulk specimens (about 100 nm thickness) were obtained at -120 °C using an ultra-microtome equipped with a diamond knife.

#### **2.3.2 Nonisothermal Crystallization Kinetics Studies using Differential Scanning Calorimetry (DSC)**

DSC experiments were performed using a Perkin Elmer, DSC-7 Instrument. The thermal history was erased by heating the samples from room temperature to 180 °C with a heating rate of 25 °C/min and then maintained at 180 °C for 2 minutes. Then measurements were

performed by cooling the samples down to room temperature at cooling rates of 2 °C/minute, 5 °C/minute, 10 °C/minute and 20 °C/minute. The protocol of the experiment is summarized below. All experiments were performed in the standard DSC mode. From the cooling curves the crystallization parameters were estimated.



### 2.3.3 Swelling Studies

Circular samples (diameter  $\approx$  2 cm) following ASTM standard of D5890 were weighed and immersed in toluene contained in test bottles with airtight stoppers kept at 80°C temperature. The samples were withdrawn periodically from the solvent and weighed on a highly sensitive electronic balance. Swollen weight is taken after reaching equilibrium state at 48 hrs.

## 3. Nonisothermal Crystallization Kinetics: Theoretical Background

Crystallization can occur at any temperature below the melting temperature  $T_m$ .  $T_m$  corresponds to the point where free energy of a polymer chain in the amorphous state and crystalline state are the same, i.e.  $G_a(T_m) = G_c(T_m)$ . The main driving force of nucleation upon cooling is the difference in the free energy of a polymer chain in crystalline state compared to that in amorphous state, i.e.  $\Delta G_m = G_a - G_c$ . Several analytical methods<sup>1-3</sup> have been developed to analyze the non-isothermal crystallization kinetics studies. The Avrami analysis, and Flynn-Wall Ozava method has been used in this work to describe the non-isothermal crystallization kinetics of XLPE/ZnO nanocomposites.

### 3.1 Avrami Equation

$$1 - X_t = \exp(-k_t t^n) \dots\dots\dots 1$$

Where  $n$  is the Avrami crystallization exponent, which depends on the nucleation mechanism and growth dimensions;  $t$  is the crystallization time;  $k_t$  is the growth rate

constant, which depends on nucleation and crystal growth; and  $X_t$  is the relative crystallinity.  $X_t$  can be defined as follows:

$$X_t = \frac{\int_{T_0}^T \frac{\partial H_c}{\partial T} dt}{\int_{T_0}^{T_\infty} \frac{\partial H_c}{\partial T} dt} \dots\dots\dots 2$$

Where  $T_0$  and  $T_\infty$  represent the onset and end of crystallization temperatures, respectively.  $\partial H_c/\partial T$  is the heat capacity.

Taking double logarithms, the equation (1) is transformed into

$$\ln[-\ln(1 - X_t)] = \ln k_t + n \ln t \dots\dots\dots 3$$

Thus, a plot of  $\ln[-\ln(1 - X_t)]$  vs  $\ln t$  enables to deduce the Avrami exponent  $n$ .

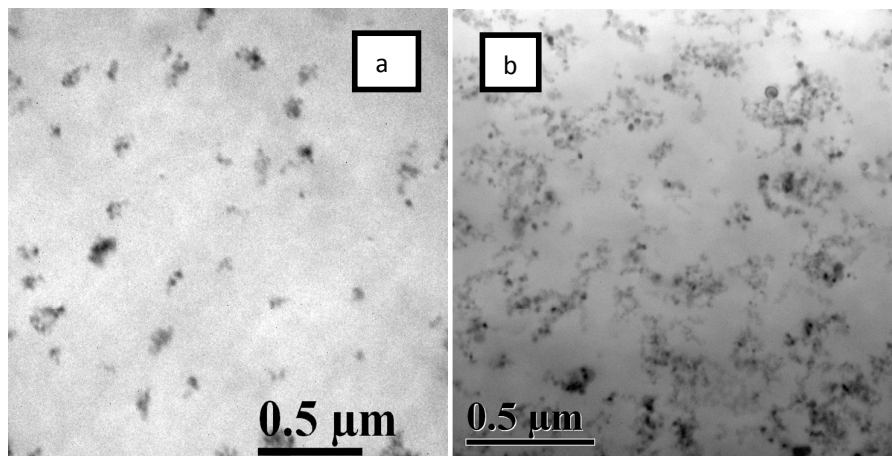
### 3.2 Flynn-Wall-Ozava Method

$$\ln(R_h/T_p^2) = (-1.052E_a/RT_p) + C \dots\dots\dots 4$$

Where  $R_h$  is the cooling rate,  $T_p$  is the iso-conversion temperature,  $E_a$  is the activation energy of the crystallization process and  $R$  is the universal gas constant.

## 4. Results and Discussion

### 4.1 Morphology



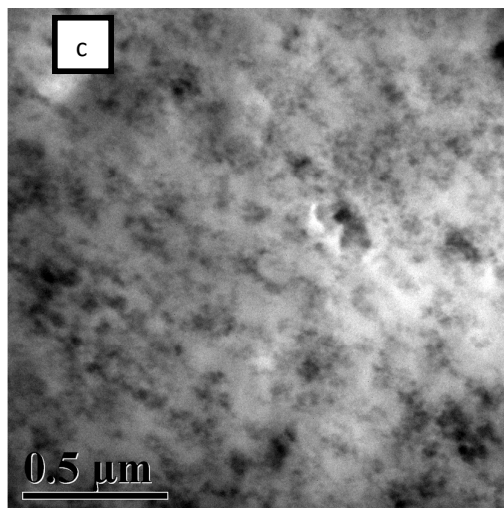


**Figure 1:** Transmission electron micrographs of, (a): XLPE/ 2 wt. % ZnO nanocomposites, (b): XLPE/ 5 wt. % ZnO nanocomposites, and (c): XLPE/ 10 wt. % ZnO nanocomposites

TEM images provide the most direct visualization of the dispersion state of ZnO particles in the nanocomposites. A typical nanocomposite dispersion micrograph is shown in Figure 1. Nanofillers are effectively dispersed in the polymeric matrix. As the filler content increases, filler-filler interaction increases and particle agglomeration is visible in the TEM images. By surface treatment on ZnO, the nanoparticle surface becomes hydrophobic in nature (more organic and nonpolar character) and this will increase the compatibility with the matrix having similar surface properties.<sup>18-19</sup> Since XLPE and nano ZnO are purely organic/inorganic system, both will be phase separated during the preparation. But the presence of alkyl group on nanoparticle act as a bridge between filler and polymer as the (-OCH<sub>3</sub>) part of trimethoxyoctyl silane will be chemically bonded to ZnO and the octyl part will form linkage with polymer leading to the enhanced interaction between polymer and filler.<sup>20-22</sup> This interactive force between nanofiller and polymer strongly supports the idea of a nucleating ability of ZnO nanofiller in this system of polymeric matrix.

Gutzow *et al.*<sup>23</sup> developed a theory to explain why inorganic particles nucleate in crystallization of linear polyolefins. Nucleating efficiency is related to the bond energies between the nucleating agent and the polymeric crystals. The organic modification on nanoparticle can increase the interaction between the fillers and the matrix. Moreover, fillers with small particle size and narrow size distribution can lead to much higher nucleation densities in the matrix. Tang *et al.*<sup>24</sup> observed an increase in the nucleation densities when the particle size of ZnO is below 100 nm and nano ZnO is the more efficient nucleating agent than micro ZnO. It is known that the existence of inorganic particles lead to the formation of crystals with less perfection and smaller size in the polymer matrix. In brief,

the TEM observation reveals the dispersion state of nanomaterials and its direct consequence on crystallization kinetics of XLPE matrix.

## 4.2 Nonisothermal Crystallization Kinetics of XLPE/ZnO Nanocomposites

### 4.2.1 Avrami Method

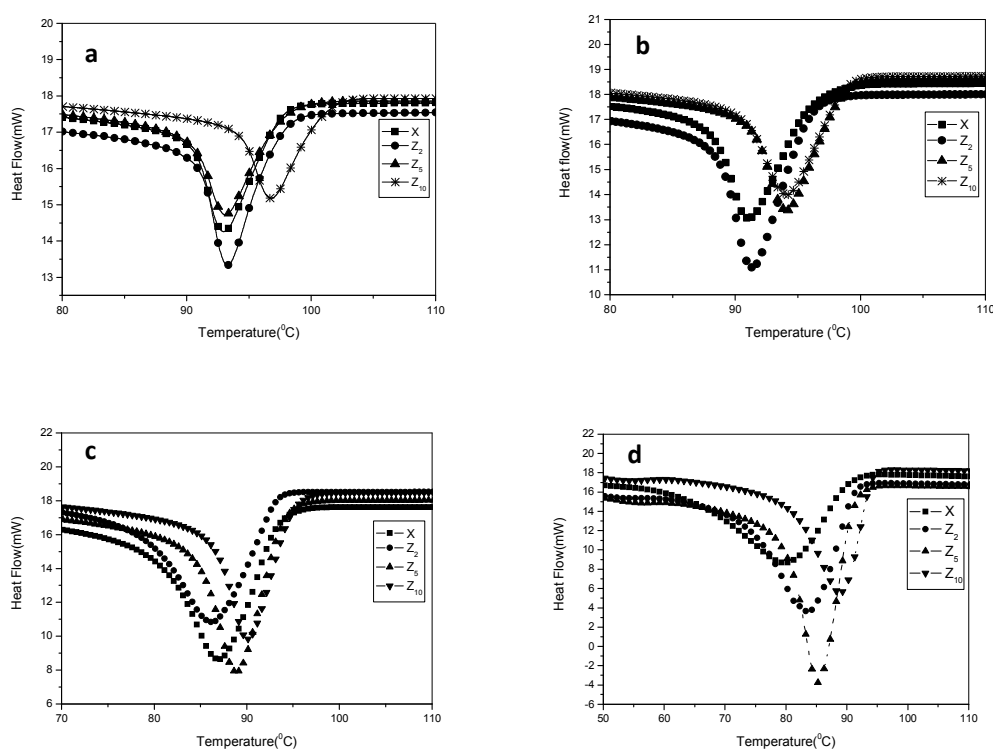
The non-isothermal crystallization curves of neat XLPE and nanocomposites at different cooling rates are compared in Figure 2. From these curves, crystallization peak temperature  $T_p$  and temperature at crystallization onset are reported in Table 1. For a given cooling rate, the early onset of crystallization and  $T_p$  increase with the nano filler concentration.

Furthermore, for each sample,  $T_p$  shifts to lower temperature, with increasing cooling rates. This could be due to the fact that, the crystallization process of polymeric molecular chain is a peristalsis process of chain segments which is driven by diffusion.<sup>14</sup> The lower the temperature, the less mobile are the polymer chains, and higher the time needed to the chain to organize into crystallites.<sup>17</sup> As a result, the extent of crystallite perfection also decreased with faster cooling rates.<sup>4</sup> Even at very fast cooling rates, the promising role of nano-particles is however able to partially compensate the negative effect of fast cooling. This can be confirmed by comparing the crystallization temperature ( $T_p$ ) values of XLPE at the lowest cooling rate of 2 °C/min (92 °C) and XLPE with 10 wt. % ZnO at the highest cooling rate of 20 °C/min (89 °C).<sup>25</sup> This shall prove the nucleating capability of ZnO nano materials in the XLPE matrix. Fillers in polymer matrix usually play dual roles, one acting as a nucleating agent to enhance crystallization, when below the percolation concentration, and the other one, acting as a hindrance to retard crystallization above the percolation concentration, because of the formed network structure associated with high melt viscosity. According to Xu *et al.*<sup>26</sup> below the percolation concentration, carbon nanotubes could largely accelerate the crystallization rates of iPP, while beyond that concentration, carbon nanotubes network might restrict the mobility and diffusion of iPP chains to crystal growth fronts and finally the crystallization rate of iPP did not change significantly. In our work the fillers always accelerate the crystallization. For the present system, percolation limit is not attained, even at 10 wt % concentration.

The relative crystallinity ( $X_t$ ) as a function of the crystallization temperature or time can be obtained by partial integration of the crystallization exotherms. The relative crystallinity  $X_t$  is calculated using equation 2, for different cooling rates as a function of temperature. As shown in Figure 3, all the  $X_t$  vs time curves at various cooling rates have same characteristic sigmoid shape. The first nonlinear part of the S shaped curve is generally considered as the nucleation step of the crystallization process. Each curve showed a linear part considered as primary crystallization; subsequently a second non linear part deviated off slightly and is considered as secondary crystallization, which is caused by the spherulitic impregnation in



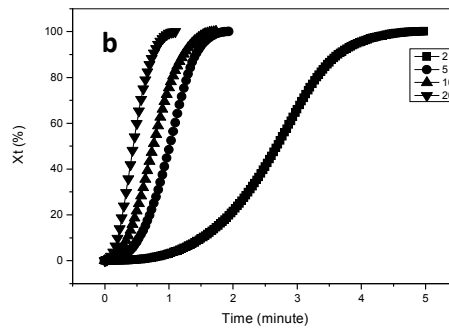
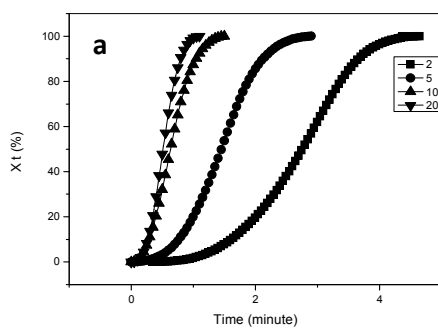
the late stage of the crystal growth.<sup>27-29</sup> While comparing  $X_t$  vs time curves, for different cooling rates, it is clear that, a higher cooling rate led to a shorter time to complete the crystallization. The half time of non-isothermal crystallization ( $t_{1/2}$ ) could be obtained from  $X_t$  vs time graph for neat XLPE and composites and the results are summarized in Table 1. It can be seen that, the value of  $t_{1/2}$  decreases with increasing cooling rate, as the crystallization proceeds faster. Moreover, at a given cooling rate, the value of  $t_{1/2}$  for XLPE/ZnO composites are lower than that for neat XLPE, signifying that the addition of nano ZnO can accelerate the overall crystallization process. The reason for this behavior might be the very dramatic increase in the nucleation density introduced by the nanoparticles in the melt of nanocomposites, as it was observed in other sort of nanocomposites.<sup>30-31</sup> As already mentioned above, Avrami exponent  $n$  can be obtained from the slope of the plot  $\ln[-\ln(1-X_t)]$  vs  $\ln t$  (eq.3) at a certain cooling rate. Such plots are displayed in Figure 4. According to the diffusion controlled growth theory<sup>16</sup>  $n = 1.5$  means that, growth of particles occurs with a nucleation rate close to zero;  $1.5 < n < 2.5$  indicates the growth of particles with constant nucleation rate and  $n > 2.5$  corresponds to the growth of small particles with an increasing nucleation rate. Based on this theory, in the present system, all the nanocomposites exhibit constant or increasing nucleation rate. For neat XLPE, only at fast cooling rates, it approaches constant nucleation rate.<sup>18, 29</sup>



**Figure 2:** Non-isothermal crystallization patterns (exothermic curves) of XLPE and nanocomposites at cooling rates 2<sup>o</sup>C/minute (a), 5<sup>o</sup>C /minute (b), 10<sup>o</sup>C /minute (c) and 20<sup>o</sup>C / minute (d)

**Table 1:** Non isothermal kinetic crystallization parameters of neat XLPE and XLPE/ZnO nanocomposites

| Sample   | Cooling rate (°C) | $T_p$ (°C) | $t_{1/2}$ (minute) | Avrami exponent $n$ | Onset Temp. (°C) |
|----------|-------------------|------------|--------------------|---------------------|------------------|
| X        | 2                 | 93         | 2.79               | 1.43                | 98               |
|          | 5                 | 90         | 1.45               | 1.44                | 97               |
|          | 10                | 87         | 0.63               | 2.5                 | 93               |
|          | 20                | 82         | 0.52               | 2.55                | 91               |
| $Z_2$    | 2                 | 93         | 2.68               | 2.45                | 99               |
|          | 5                 | 92         | 0.99               | 3.1                 | 99               |
|          | 10                | 86         | 0.60               | 2.98                | 94               |
|          | 20                | 84         | 0.42               | 2.38                | 92               |
| $Z_5$    | 2                 | 93         | 2.50               | 2.35                | 99               |
|          | 5                 | 94         | 0.97               | 2.78                | 99               |
|          | 10                | 89         | 0.58               | 2.73                | 95               |
|          | 20                | 84         | 0.31               | 2.78                | 92               |
| $Z_{10}$ | 2                 | 97         | 2.54               | 2.74                | 102              |
|          | 5                 | 94         | 1.01               | 3.06                | 99               |
|          | 10                | 90         | 0.57               | 2.48                | 96               |
|          | 20                | 89         | 0.30               | 2.98                | 95               |



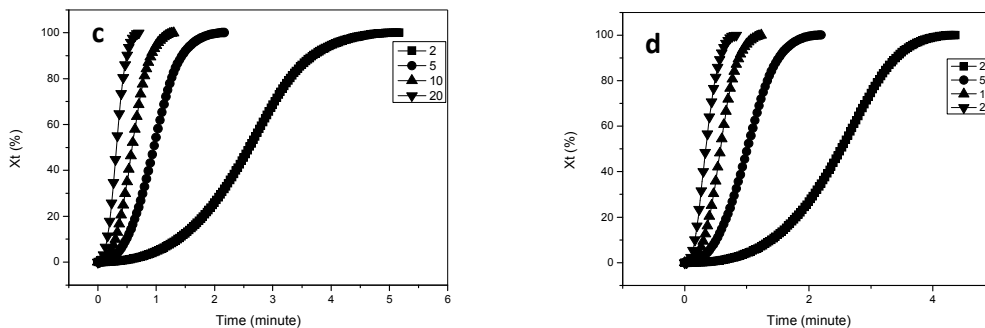


**Figure 3:** Patterns of  $X_t$  vs time for XLPE(a), XLPE/2 wt. % ZnO nanocomposite (b), XLPE/ 5 wt. % ZnO nanocomposite (c) and XLPE/10 wt. % ZnO nanocomposite (d)

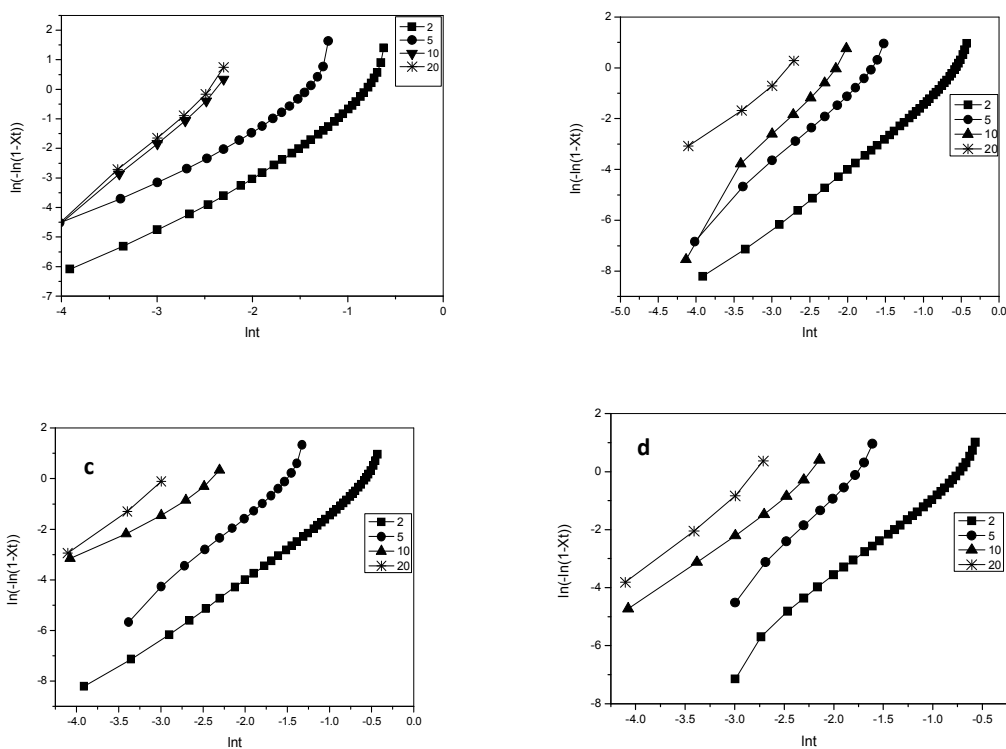


**Figure 4:** Patterns of  $\ln[-\ln(1-X_t)]$  vs  $\ln t$  for XLPE (a), XLPE/2 wt. % ZnO nanocomposite (b), XLPE/ 5 wt. % ZnO nanocomposite (c) and XLPE/10 wt. % ZnO nanocomposite (d)

#### 4.2.2 Flynn-Wall-Ozava Method

##### Activation Energy

Any crystal growth process can be characterized by two types of activation energies, the activation energy for nucleation and activation energy for growth. Usually, the two energy barriers are considered to be condensed into a single energy barrier, since usually these two

processes are separated by very low barriers. Crystallization activation energy of XLPE and nanocomposites were determined using Flynn-Wall Ozava approach. Flynn-Wall Ozava plot is presented in Figure 5 and the activation energy values ( $E_a$ ) are listed in Table 2. The  $E_a$  values of all the nanocomposites are significantly lower than that of neat XLPE, which refers the reduction in energy barrier for crystallization. The addition of nanomaterials caused a decrease in the  $E_a$  which made the molecular chains of polyethylene easier to crystallize and thus there is an increase in rate of crystallization.<sup>2, 24</sup> The decrease in  $E_a$  could be due to the fact that this energy is the sum of two components: one term corresponding to the nucleation and the other to the growth. When crystallization progresses, the energy required for nucleation can progressively disappear and then  $E_a$  can decrease.<sup>32</sup> Hao *et al.*<sup>19</sup> reported the same trend of activation energy values with respect to the filler concentration for PP/Si<sub>3</sub>N<sub>4</sub> nanocomposites.

**Table 2:** Activation energy values (Flynn-Wall-Ozava method), and values of melting temperature, enthalpy of fusion ( $\Delta H_f$ ), percentage crystallinity and lamellar thickness

| Sample          | Activation Energy(KJ/mol) Flynn-Wall-Ozava method | Melting Temperature (°C) | $\Delta H_f$ (J/g) | % Crystallinity ( $X_c$ ) | Lamellar thickness( $A^0$ ) |
|-----------------|---------------------------------------------------|--------------------------|--------------------|---------------------------|-----------------------------|
| X               | 265                                               | 102.48                   | 109                | 38                        | 60.60                       |
| Z <sub>2</sub>  | 255                                               | 102.22                   | 119                | 43                        | 59.80                       |
| Z <sub>5</sub>  | 258                                               | 100.62                   | 120                | 44                        | 56.30                       |
| Z <sub>10</sub> | 253                                               | 99.38                    | 110                | 43                        | 57.87                       |

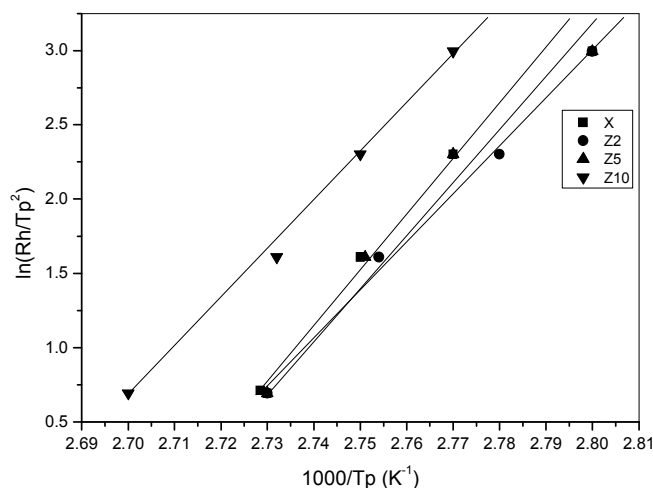


**Figure 5:** Flynn-Wall-Ozava plots of XLPE and nanocomposites

### 4.3 Crystallization and crystal morphology

Percentage crystallinity  $X_m$  is defined by the ratio between  $\Delta H_m/(1-\chi)$  (where  $\chi$  is the content of nano ZnO ) and the heat of fusion of purely crystalline form of PE  $\Delta H_m^0 = 289.9\text{J/g}$ .

$$X_m = [\Delta H_m/(1-\chi)]/ \Delta H_m^0 \dots\dots\dots 5$$

Lamellar thickness is estimated using Gibbs-Thomson equation as

$$T_m(D)/T_m(\alpha) = 1-(2\gamma V_m/H_m D) \dots\dots\dots 6$$

Where  $T_m(D)$  is the melting temperature of a lamellar crystal with a thickness of  $D$ ,  $T_m(\alpha)$  denotes the corresponding bulk value,  $g$  is the interface energy of the lamellar crystal and the surroundings,  $V_m$  is the molar volume of the crystal, and  $H_m$  is molar melting enthalpy [1].

The melting temperature, percentage crystallinity values and lamellar thickness are compared in Table 2. The ZnO nanoparticle can act as a nucleating agent in nanocomposites. At the nano dimension scale, the nano particle can substitute for the absence of primary nuclei thus competing with the confined crystallization. At 2 wt% nanofiller concentration itself nucleating ability of ZnO nanoparticle improves the crystallinity considerably. As the nanofiller contributes more towards nucleation, lamellar thickening shows a decreasing trend. The position of melting peak temperature is related to the size of the crystal and the  $\Delta H$  value is in direct correlation with percentage crystallinity and number of spherulites. The melting peak becomes broader with increasing nano ZnO concentration. This should be due to the combination of the different cross linking degree and the filler's nucleation and disturbance effect.<sup>33</sup>

The driving force for larger lamellar thickness is the larger free energy change during crystallization. In order to initiate the crystallization process, a section of chains need to be deposited on the crystal growth front. The localization of chains on the crystal surface is associated with a decrease in entropy of the polymer chain. This leads to an entropic barrier that increases with crystal thickness. The growth rate therefore is the result of an interplay between the energy barrier and the driving force *ie.* the change in free energy. The actual thickness of lamellar crystals corresponds to the thickness of crystals that have the largest growth rate under given experimental conditions. It should be noted that, both the energy barrier and the driving force are under cooling rate dependent. Besides, under cooling, other factors such as the chain length and the concentration of defects on the chain backbone also have a significant influence on the growth rate and the final morphology.<sup>34-35</sup>

Crystallization kinetics and spherulitic growth rate can be strongly influenced by the presence of amorphous cross linked portion. In general the crystallization process consists

of two major stages: nucleation and crystal growth. Nucleation is the primary step. The crystal growth, subsequent to lamellar thickening into spherulitic structure can be hindered by cross links.<sup>36</sup> In the present system, small sized, more number of crystal fraction formation contribute towards the net crystal morphology.

#### 4.4 Crystallization in a cross linked system

The nano materials, the added foreign phase, which presents a new surface on which crystal growth can occur.<sup>37-38</sup> Since the polymer chain system is densely packed, center of mass motions of one chain segment necessarily involve coordinated motions of other segments. The length scale of these coordinated motions can be measured by various means and is typically in the range of 2-4 nm for polymeric systems. The mutual chain rearrangement between the adjacent crystals is a cooperative phenomenon where certain localized chain segments are involved rather than the whole chain.<sup>39</sup> This coordinated motions, suggests the complex mechanism of crystallization in a cross linked structure. The  $t_{1/2}$  value of crystallization is less for nanocomposites, which indicates that the cross linked structure, has less affect on the kinetics of crystallization, as it is proceeded by coordinated motions of polymer chains.

According to the theory of swelling of cross-linked polymers, strong bonds, such as the chemical cross links between the XLPE chains, prevent the molecules becomes completely surrounded by the fluids, but cause swelling. Cross link density is frequently calculated from equilibrium swelling data by means of the Flory-Rehner equation<sup>40-41</sup> and this equation relating swelling behavior to the kinetic theory through the polymer-solvent interaction parameter or Huggins factor.

According to Flory-Rehner equation  $V=1/2M_c$ ..... 7

Where  $V$  is the cross link density ( $\text{mol}/\text{cm}^3$ ) and  $M_c$  is the molecular weight of polymer between cross links.

$$M_c = \frac{[-\rho_r \cdot V_s \cdot V_{rf}^{1/3}]}{[\ln(1-V_{rf}) + V_{rf} + \chi \cdot V_{rf}^2]} \dots\dots\dots 8$$

Where  $\rho_r$  is the density of polymer,  $V_s$  is the molar volume of solvent and  $V_{rf}$  is the volume fraction of polymer in the solvent-swollen sample and is given by:

$$V_{rf} = \frac{[(d-fw)/\rho_r]}{[(d-fw)/\rho_r + (A_s/\rho_s)]} \dots\dots\dots 9$$

Where  $d$  is the deswollen weight,  $f$  is the volume fraction of the filler,  $w$  is the initial weight

of the sample,  $A_s$  is the amount of solvent absorbed, and  $\rho_s$  is the density of solvent. In equation (8),  $\chi$  is the interaction parameter and is given by Hildebrand equation.

$$\chi = \beta + \frac{V_s (\rho_s - \rho_p)^2}{RT} \dots\dots\dots 10$$

Where  $\beta$  is the lattice constant, R is the universal gas constant, T is the absolute temperature, and  $\rho_p$  is the solubility parameter of polymer.

**Table 3:** Cross-link density values and theoretical and experimental values of  $M_c$  of XLPE and nanocomposites

| Sample | Cross-link density<br>( $10^{-4}$ mol/cm <sup>3</sup> ) | $M_c$ (expt) | $M_c$ (aff) | $M_c$ (ph) |
|--------|---------------------------------------------------------|--------------|-------------|------------|
| X      | 1.11                                                    | 4497         | 1778        | 2234       |
| Z1     | 1.18                                                    | 4233         | 1569        | 2163       |
| Z2     | 1.50                                                    | 3304         | 1447        | 2044       |
| Z3     | 0.85                                                    | 5926         | 1915        | 1914       |

Cross-link density values are summarized in Table 3. Usually, crystallization rate decreases with cross linking. In our case, cross link density is not much varying till 5 wt % of filler loading (only slight variation). This indicates that, filler contributes less towards the crosslink density of the system. Its major contribution is in nucleation and due to this, we are getting crystallization kinetic parameters much improved (faster kinetics) compared to neat XLPE. Crystallization peak temperature and  $t_{1/2}$  values indicate faster crystallization kinetics. For the sample Z<sub>10</sub>, with the higher filler loading, cross-link density is decreased due to the predominant filler/filler interaction over filler/polymer interaction. In that situation, nucleation is dominating and the kinetics is much faster for Z<sub>10</sub> samples.

To compare the experimental results with the theory, the molecular weight between the cross links was compared with the affine limit of the model [ $M_c$ (aff)] and the phantom network model proposed by James and Guth using the equation Eqs. (12) and (13), respectively. In the affine network model, the cross-link junctions do not fluctuate around a mean position and they move affinely with strain. The mean square fluctuations in junction positions are zero. The phantom network model assumes that network chains can freely pass through each other *i.e.* the junction points of the cross links can fluctuate. The mobility

of the cross-link junction is of crucial importance in the dynamics of cross links and the polymer chain orientation.<sup>42</sup>

$$M_c(\text{aff}) = [\rho_p \nu \phi_{2c}^{2/3} \phi_{2m}^{1/3} (1 - (\mu/\nu) \phi_{2m}^{1/3})] / [-\ln(1 - \phi_{2m}) + \phi_{2m} + \chi \phi_{2m}^2] \dots \dots \dots 11$$

$$M_c(\text{Ph}) = [(1 - 2/\chi) \rho_p \nu \phi_{2c}^{2/3} \phi_{2m}^{1/3}] / [-\ln(1 - \phi_{2m}) + \phi_{2m} + \chi \phi_{2m}^2] \dots \dots \dots 12$$

Where  $\mu$  and  $\nu$  are the number of effective chains and junctions.  $\phi_{2m}$  is the polymer volume fraction of swelling at equilibrium, and  $\phi_{2c}$ , the polymer volume fraction during crosslinking, where the chain may move freely through one another where  $\chi$  is the junction functionality. The calculated  $M_c$  values along with the experimental values are detailed in Table 3. It was found that the  $M_c$  values of phantom network model showed moderate agreement with the experimental values rather than with the affine model. Here the chain can move freely through one another, *i.e.* the junction points fluctuate over time around their mean position without any hindrance from the neighbouring molecules.<sup>43</sup>

From the results, it can be concluded that the system agree with the Phantom model and thus the fluctuations in cross link junctions are allowed. This may be the favouring factor in crystallization mechanism of this cross linked system.

#### 4.5 Nucleation Activity

The evaluation of non isothermal crystallization behaviour, with respect to nucleation activity, demonstrates the success of nucleating ability of ZnO nanoparticles in the XLPE system. Nucleation activity is a measurement of the work decrement of three-dimensional nucleation with the addition of a foreign substrate. Dobrev and Gutzow introduced a simple method for calculating the nucleation activity of foreign substrates in polymer melt.

According to Dobrev and Gutzow<sup>23</sup>, the nucleation activity of foreign substrates in polymer melts can be calculated from the ratio:

$$\psi = B^*/B \dots \dots \dots 13$$

Where  $B^*$  stands for the parameter during heterogeneous nucleation, while  $B$  stands for that in homogeneous nucleation.  $B$  and  $B^*$  can be experimentally determined from the slope of the following equation:

$$\ln R = \text{Constant} - B/\Delta T_p^2 \dots \dots \dots 14$$

Where  $\Delta T_p$  represents the supercooling ( $\Delta T_p = T_m - T_p$ ).

Plots of  $\ln R$  versus  $1/\Delta T_p^2$  for neat XLPE and all nanocomposites are shown in Figure 6.



If the foreign substrate is extremely active  $\psi$  approaches 0, while for inert particles,  $\psi$  approaches 1. From the graph, it can be seen that  $\psi$  values for nanocomposites are lower than that of neat XLPE, indicating that, ZnO nanoparticles are acting effectively as a nucleation agent in the XLPE matrix. Nucleation activity shows a positive trend with the amount of nanofiller added. In the present system, nano ZnO can perform as a good nucleating agent, thus accelerating the non-isothermal crystallization of the XLPE nanocomposites.

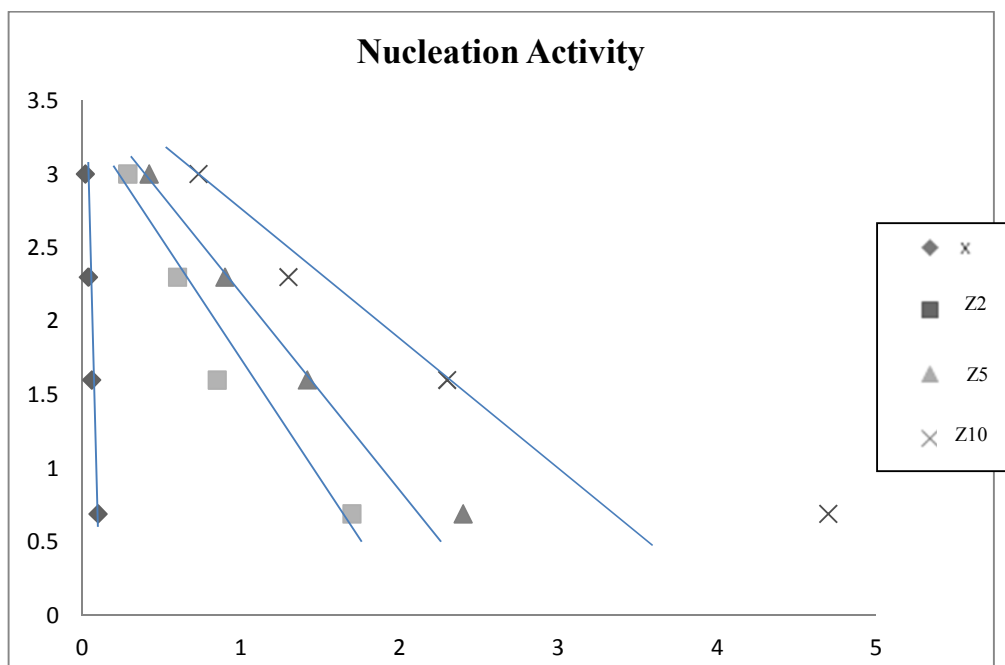


**Figure 6:** Plots of  $\ln R$  versus  $1/\Delta T_p^2$  ( $\Delta T_p = T_m - T_p$ ) for neat XLPE and XLPE/ZnO nanocomposites

## 5. Conclusions

In this work, the non isothermal crystallization kinetics, crystal morphology and the parameters contributing in crystallization mechanism have been investigated with special reference to the nucleating capability of ZnO nanoparticles in a complex system of cross-linked polyethylene. The results can be summarized as follows:

1. The TEM observation reveals the fine dispersion of nanomaterials, and this microstructural development accelerates crystallization kinetics of XLPE matrix.
2. It can distinctly be observed that, for a given cooling rate, the early onset of crystallization results and an increasing trend of  $T_p$ , is directly proportional to the

nano filler concentration. It is the indication of the direct correlation of number of nucleating sites and crystallization phenomena.

3. At a given cooling rate, the value of  $t_{1/2}$  for XLPE/ZnO composites are lower than that for neat XLPE, signifying that the addition of nano ZnO can accelerate the over all crystallization process.
4. According to the diffusion controlled growth theory, all the nanocomposites exhibit constant nucleation rate or the growth of small particles with an increasing nucleation rate.
5. The activation energy obtained from Flynn-Wall Ozava plot shows that, the  $E_a$  values of all the nanocomposites are lower than neat XLPE, which refers the reduction in energy barrier for crystallization.
6. The percentage crystallinity values and the theoretical estimation of nucleation activity prove the heterogeneous nucleating ability of ZnO nanoparticles in XLPE system.
7. In the present system, nucleation, the rate determining step plays important role instead of crystal growth process by secondary and tertiary growth mechanism.

## 6. References

- (1) D. Olmos, C. Dominguez, P. D. Castrillo, Gonzalez-Benito, *J. Polymer*, 2009, **50**, 1732-1742
- (2) S. H. Abbasi, I. A. Hussein, M. A. Parvez, *Journal of Applied Polymer science*, 2011, **119**, 290-299
- (3) Z. Wang, X. Wang, Z. Zhang, *Journal of Dispersion Science and Technology*, 2009, **30**, 1231-1236
- (4) K. R. Patnaik, K. Sirisha Devi, V. K. Kumar, *International Journal of Chemical Engineering and Applications*, 2010, **1**
- (5) B. Wunderlich, *Macromolecular physics*, New York: Academic Press; 1973
- (6) J. Kraus, P. Muller-Buschbaum, T. Kuhlmann, D. W. Schubert, M. Stamm, *Europhysics Lett.* 2000, **49**, 210-216
- (7) R. S. Paipanandiker, J. R. Dorgan, T. Pakula, *Macromolecules*, 1997, **30**, 6348-6352
- (8) J. Baschnagel, T. Meyer, T. Varnik, S. Metzger, M. Aichele, M. Muller, *Interface Sci*, 2003, **11**, 159-173
- (9) H. Meyer, J. Baschnagel, *Eur. Phys. J. E.*, 2003, **12**, 147-151
- (10) J. Shen, H. Zou, S. Wu, *Chem. Rev.* 2008, **108**, 3893-3957
- (11) P. Russo, D. Acierno, G. Filippone, G. Romeo, *Macromol. Symp.* 2007, **24**, 59-66
- (12) X. Huang, F. Liu, P. Jiang, *IEEE Transactions on Dielectrics and Electrical Insulation*, 2010, **17**, 1697-1704
- (13) Z. Qiu, Z. Li, *Ind. Eng. Chem. Res*, 2011, **50**, 12299-12303
- (14) K. Chen, J. Yu, Z. Oiu, *Ind. Eng. Chem. Res*, 2013, **52**, 1769-1774

- (15) J. Yu, Z. Qiu, *ACS Appl. Mater. Interfaces*, 2011, **3**, 890-897
- (16) H. Bai, W. Zhang, H. Deng, Q. Zhang, Q. Fu, *Macromolecules*, 2011, **44**, 1233-1237
- (17) M. S. Sreekala, J. George, M. G. Kumaran, S. Thomas, *Comp. Sci. Tech.* 2002, **62**, 339
- (18) J. P. Jose, V. Mhetar, S. Culligan, S. Thomas, *Science of advanced Materials*, 2013, **5**, 1-12
- (19) W. Hao, W. Yang, W. Cai, Y. Huang, *Polymer Testing*, 2010, **29**, 527-533
- (20) X. Zhang, L. C. Simon, *Macromol. Mater. Eng.* 2005, **290**, 573-583
- (21) J. A. Pople, G. R. Mitchell, S. J. Sutton, A. S. Vaughan, C. K. Chai, *Polymer*, 1999, **40**, 2769-2777
- (22) N. Guo, S. A. DiBenedetto, P. Tewari, T. Lanagan, M. A. Ratner, Marks, *Chem. Mater.* 2010, **22**, 1567-1578
- (23) A. Dobрева, A. Stoyano, J. Gutzow, *Appl. Polym. Symp.*, 1991, **48**, 473
- (24) G. J. Tang, Y. Wang, H. Y. Liu, L. A. Belfiore, *Polymer*, 2004, **45**, 2081
- (25) W. Guan, Z. Qiu, *Ind. Eng. Chem. Res.*, 2012, **51**, 3203-3208
- (26) W. Xu, H. Zhai, H. Guo, N. Whitely, W. P. Pan, *Journal of Thermal Analysis and Calorimetry*, 2004, **78**, 1-12
- (27) C. Jiao, Z. Wang, X. Liang, Y. Hu, *Polymer Testing*, 2005, **24**, 71-80
- (28) S. A. Madbouly, *Journal of Macromolecular Science, Part B: Physics*, 2011, **50**, 427-443
- (29) J. C. Qiao, J. M. Pelletier, *Journal of Non-Crystalline Solids*, 2011, **357**, 2590-2594
- (30) W. Hao, W. Yang, H. Cai, Y. Huang, *Polymer Testing*, 2010, **29**, 527-533
- (31) K. Jeao, L. Lumata, T. Tokumoto, E. Steven, J. Brooks, R. G. Alamo, *Polymer*, 2007, **48**, 4751-4764
- (32) R. Haggemueller, J. E. Fischer, K. I. Winey, *Macromolecules*, 2006, **39**, 2964-2971
- (33) X. Wang, J. Zhao, M. Chen, L. Ma, X. Zhao, Z. Dang, Z. Wang, *J. Phys. Chem. B.* 2013, **117**, 1467-1474
- (34) J. C. Qiao, J. M. Pelletier, *Trans. Nonferrous Met. Soc. China*, 2012, **22**, 577-584
- (35) J. D. Hoffmann, R. L. Miller, H. Marand, D. B. Roitman, *Macromolecules*, 1992, **25**, 2221
- (36) S. Rastogi, A. B. Spoelstra, J. G. P. Goossens, P. J. Lemstra, *Macromolecules*, 1997, **30**, 7880-7889
- (37) G. J. Tang, Y. Wang, H. Y. Liu, L. A. Belfiore, *Polymer*, 2004, **45**, 2081
- (38) A. Deepak Ph. D Thesis, University of Massachusetts – Amherst, 2010
- (39) X. Huang, F. Liu, P. Jiang, *IEEE Transactions on Dielectrics and Electrical Insulation*, 2010, **17**, 1697-1704
- (40) J. A. Pople, G. R. Mitchell, S. J. Sutton, A. S. Vaughan, C. K. Chai, *Polymer*, 1999, **40**, 2769-2777
- (41) S. N. Bhattacharya, D. S. Choudhary, R. Prasad, R. K. Gupta, *Thermochimica Acta*, 2005, **433**, 187-195
- (42) R. Wilson, S. M. George, H. J. Maria, S. T. Plivelic, A. Kumar, S. Thomas, *J. Phys. Chem. C.* 2012, **116**, 2002-2014

- (43)H. J. Maria, N. Lyczko, A. Nzihou, C. Mathew, S. C. George, K. Joseph, S. Thomas, *J. Mater. Sci*, 2013, **48**, 5373-5386

